

## Embolism resistance in stems of herbaceous Brassicaceae and Asteraceae is linked to differences in woodiness and precipitation

Larissa Chacon Dória<sup>1,\*</sup>, Cynthia Meijs<sup>1</sup>, Diego Sotto Podadera<sup>2</sup>, Marcelino del Arco<sup>3</sup>, Erik Smets<sup>1</sup>, Sylvain Delzon<sup>4</sup> and Frederic Lens<sup>1</sup>

<sup>1</sup>Naturalis Biodiversity Center, Leiden University, PO Box 9517, 2300 RA Leiden, The Netherlands, <sup>2</sup>Programa de Pós-Graduação em Ecologia, UNICAMP, Campinas, São Paulo, Brazil, <sup>3</sup>Department of Plant Biology (Botany), La Laguna University, 38071 La Laguna, Tenerife, Spain and <sup>4</sup>BIOGECO INRA, Université Bordeaux, 33615 Pessac, France

\* For correspondence. E-mail: [larissa.chacondoria@naturalis.nl](mailto:larissa.chacondoria@naturalis.nl)

Received: 30 June 2018 Returned for revision: 30 October 2018 Editorial decision: 26 November 2018 Accepted: 5 December 2018

- **Background and Aims** Plant survival under extreme drought events has been associated with xylem vulnerability to embolism (the disruption of water transport due to air bubbles in conduits). Despite the ecological and economic importance of herbaceous species, studies focusing on hydraulic failure in herbs remain scarce. Here, we assess the vulnerability to embolism and anatomical adaptations in stems of seven herbaceous Brassicaceae species occurring in different vegetation zones of the island of Tenerife, Canary Islands, and merged them with a similar hydraulic–anatomical data set for herbaceous Asteraceae from Tenerife.
- **Methods** Measurements of vulnerability to xylem embolism using the *in situ* flow centrifuge technique along with light and transmission electron microscope observations were performed in stems of the herbaceous species. We also assessed the link between embolism resistance vs. mean annual precipitation and anatomical stem characters.
- **Key Results** The herbaceous species show a 2-fold variation in stem  $P_{50}$  from  $-2.1$  MPa to  $-4.9$  MPa. Within *Hirschfeldia incana* and *Sisymbrium orientale*, there is also a significant stem  $P_{50}$  difference between populations growing in contrasting environments. Variation in stem  $P_{50}$  is mainly explained by mean annual precipitation as well as by the variation in the degree of woodiness (calculated as the proportion of lignified area per total stem area) and to a lesser extent by the thickness of intervessel pit membranes. Moreover, mean annual precipitation explains the total variance in embolism resistance and stem anatomical traits.
- **Conclusions** The degree of woodiness and thickness of intervessel pit membranes are good predictors of embolism resistance in the herbaceous Brassicaceae and Asteraceae species studied. Differences in mean annual precipitation across the sampling sites affect embolism resistance and stem anatomical characters, both being important characters determining survival and distribution of the herbaceous eudicots.

**Key words:** Canary Islands, drought, embolism resistance, herbaceous species, stem anatomy, thickness of intervessel pit membranes, woodiness, xylem hydraulics.

### INTRODUCTION

Hydraulic failure is one of the main physiological mechanisms associated with reductions in forest productivity and drought-induced tree mortality (Choat *et al.*, 2012; Anderegg *et al.*, 2016; Adams *et al.*, 2017). Water movement inside the conduits is prone to dysfunction due to negative xylem pressures generating metastable conditions (Tyree and Sperry, 1989; Tyree and Zimmermann, 2002). With increasing drought stress, embolisms could propagate from a gas-filled conduit to a neighbouring functional conduit through interconduit pit membranes, potentially generating lethal levels of embolisms (Tyree and Zimmermann, 2002; Brodribb *et al.*, 2010; Brodersen *et al.*, 2013). The vulnerability to xylem embolism can be measured by vulnerability curves, in which the percentage loss of hydraulic conductivity is plotted against the xylem pressure (Cochard *et al.*, 2010, 2013). The  $P_{50}$  value, referring to the negative pressure associated with 50 % loss of hydraulic conductivity, is an oft-cited proxy for plant drought resistance,

although it does not present a critical threshold value for angiosperms (Urli *et al.*, 2013; Adams *et al.*, 2017).

There is considerable interspecific variation in  $P_{50}$  across plant species, from  $-0.5$  MPa up to  $-19$  MPa, and the majority of studies show that species from dry environments are generally more resistant to embolism (more negative  $P_{50}$ ) than species from wet environments (Choat *et al.*, 2012; Lens *et al.*, 2013, 2016; Larter *et al.*, 2015). Knowledge about intraspecific variation in  $P_{50}$  remains scarce and provides contradictory results: it seems to be species specific, but it can vary either considerably (Kolb and Sperry, 1999; Choat *et al.*, 2007; Corcuera *et al.*, 2011; Nolf *et al.*, 2014, 2016; Volaire *et al.*, 2018; Cardoso *et al.*, 2018) or subtly (Holste *et al.*, 2006; Martínez-Vilalta *et al.*, 2009; Lamy *et al.*, 2013; Ahmad *et al.*, 2017), or may even be absent (Maherali *et al.*, 2009; Wortemann *et al.*, 2011) for woody as well as for herbaceous species.

There is a vast body of literature available focusing on hydraulic conductivity and safety for hundreds of woody species

(Maherali *et al.*, 2004; Pittermann *et al.*, 2010; Choat *et al.*, 2012; Bouche *et al.*, 2014; Gleason *et al.*, 2016). Herbs, on the other hand, remain poorly investigated:  $P_{50}$  values of stems are available for <30 species, of which a minority are eudicots while most species are grasses (e.g. Mencuccini and Comstock, 1999; Stiller and Sperry, 2002; Kocacinar and Sage, 2003; Holste *et al.*, 2006; Maherali *et al.*, 2009; Rosenthal *et al.*, 2010; Lens *et al.*, 2013, 2016; Nolf *et al.*, 2014, 2016; Skelton *et al.*, 2017; Dória *et al.*, 2018; Volaire *et al.*, 2018). Based on this limited data set, most herbaceous species studied so far are sensitive to embolism formation in their stems, with a  $P_{50}$  of around  $-2.5$  MPa. However, some of the grass stems studied are remarkably resistant to embolism formation (up to  $-7.5$  MPa), implying that both herbs and trees share the ability to support very negative water potentials without embolism formation during drought stress (Lens *et al.*, 2016).

In this study, we focus on the research field of xylem hydraulics in herbaceous stems which has been largely neglected, despite the overwhelming occurrence of economically important herbaceous food crops (Monfreda *et al.*, 2008) and the dependency on grazed grasslands for our livestock. The main reason for neglecting herb hydraulics is that their fragile stems and often low hydraulic conductance make vulnerability curves technically more challenging. However, recent fine-tuning of the high-throughput *in situ* flow centrifuge method (cavitron; Lens *et al.*, 2016; Dória *et al.*, 2018) and the new optical vulnerability technique (Skelton *et al.*, 2017) have yielded stem  $P_{50}$  data of herbaceous species, which opens up new opportunities to boost the virtually neglected aspect of herb hydraulics and predict future crop productivity and survival (Challinor *et al.*, 2009), especially in a world facing climate change (Rahmstorf and Coumou, 2012; Dai, 2013).

In addition to the understudied aspect of herb hydraulics, we also investigate stem anatomical characters to assess poorly known structure–function relationships in herbaceous stems. Plant sensitivity to drought-induced embolism is determined by a whole suite of stem anatomical characters in woody trees (Hacke and Jansen, 2009; Lens *et al.*, 2011; Jacobsen *et al.*, 2012; Pivovarov *et al.*, 2016; Pereira *et al.*, 2017; O'Brien *et al.*, 2017), of which the thickness of intervessel pit membranes is probably one of the most hydraulically relevant anatomical features, altering both water flow efficiency and the spread of potential lethal levels of embolism in the xylem (Jansen *et al.*, 2009; Lens *et al.*, 2011; Li *et al.*, 2016; Gleason *et al.*, 2016; Dória *et al.*, 2018). Furthermore, vessel diameter is an informative character determining xylem area-specific conductivity ( $K_s$ ) (Hacke *et al.*, 2016), but also correlates with plant height, environmental constraints and, potentially, embolism resistance (Davis *et al.*, 1999; Olson and Rosell, 2013; Schreiber *et al.*, 2015; Hacke *et al.*, 2016; Olson *et al.*, 2018). Mechanical characters such as wood density, total degree of lignification, thickness-to-span ratio of vessels and thickness of the intervessel wall have also been linked to increasing drought stress resistance (Hacke *et al.*, 2001; Jacobsen *et al.*, 2005, 2007; Chave *et al.*, 2009; Hoffman *et al.*, 2011; Pratt and Jacobsen, 2017). These mechanical characters are often reported as indirectly linked to embolism resistance, since embolism formation and spread occur at the pit level (Bouche *et al.*, 2014; Pereira *et al.*, 2017; Dória *et al.*, 2018).

In herbaceous eudicots, an increase in embolism resistance is linked to an increase in wood formation, which reflects an

increase in the proportion of lignified area per total stem area (Lens *et al.*, 2013, 2016; Tixier *et al.*, 2013; Dória *et al.*, 2018), and also grasses that are more resistant to embolism formation have more lignified stems compared with the more vulnerable species (Lens *et al.*, 2016). Wood formation has been observed in many herbaceous eudicots, especially at the base of the stem, and several studies show a continuous range in the degree of wood formation between stems of herbaceous eudicot species (Dulin and Kirchoff, 2010; Schweingruber *et al.*, 2011; Lens *et al.*, 2012a; Kidner *et al.*, 2016; Dória *et al.*, 2018). This highlights the fuzzy boundaries between woodiness and herbaceousness, leading to intermediate life forms such as ‘woody herbs’ or ‘half shrubs’ (Lens *et al.*, 2012a), but species with these intermediate life forms do not form a wood cylinder that extends towards the upper parts of the stem and are therefore considered as herbaceous (Kidner *et al.*, 2016).

In this study, we combine hydraulic measurements with detailed stem anatomical characteristics and climatic variables (from meteorological stations near the sampling sites) to investigate structure–function relationships in stems of seven herbaceous species belonging to the Brassicaceae family from the island of Tenerife (Canary Islands, Spain), and merged this data set with a similar data set for four herbaceous Asteraceae species that were sampled on the same island for a previous publication (Dória *et al.*, 2018). The main reason for selecting Tenerife is the huge range of climatic conditions in a small area of 2034 km<sup>2</sup>, ranging from the humid northern laurel forests of Anaga to the dry southern desert-like region around El Médano, separated by the tall Teide volcano (approx. 3700 m asl) generating different altitudinal vegetation types (del-Arco *et al.*, 2006). We address the following questions. (1) Do herbaceous species growing in drier environments have more embolism-resistant stems, both across and within species? (2) What are the stem anatomical characters that explain the variation in embolism resistance amongst the species studied? (3) Is there any relationship between precipitation and both xylem vulnerability to embolism and anatomical characters?

## MATERIALS AND METHODS

### *Plant material and climate data*

We collected the Brassicaceae specimens throughout the island of Tenerife, in different vegetation zones with different mean annual precipitation and aridity indices. The climatic data of precipitation and temperature for each of the sampling sites were provided by Agencia Estatal de Meteorología (AEMET, Spanish Government), covering a period from 110 to 30 years depending on the meteorological station. We received the data from five different meteorological stations (Anaga San Andrés, Arico Bueno, Arafo, Laguna Instituto and Vilaflor) matching the five sampling sites (Supplementary Data Fig. S1). We used the mean annual precipitation for each site, and calculated the potential evapotranspiration using the Thornthwaite equation (1948). The aridity indices were calculated as a ratio of mean annual precipitation to mean annual potential evapotranspiration (UNEP, 1997). Since this aridity index is highly correlated with mean annual precipitation ( $P < 0.001$ ,  $r = 0.993$ ) we opted to select the former in the statistical models.

The collection trip was carried out in March 2017, matching with the wet, flowering period of the herbaceous species. We harvested seven annual Brassicaceae species: *Hirschfeldia incana* (L.) Lagr.-Fossat, *Raphanus raphanistrum* L., *Rapistrum rugosum* L. All., *Sinapis alba* L., *Sinapis arvensis* L., *Sisymbrium erysimoides* Desf. and *Sisymbrium orientale* L. The time of germination is similar for all species studied and it is linked to the arrival of the rains in autumn and winter. However, there can be small differences between populations, amongst and within species: populations growing on the northern slopes of the island generally germinate earlier than plants growing on the southern slopes due to the moist north-eastern trade winds, and populations from higher altitudes usually germinate later than plants from lower altitudes.

The specimens of *H. incana* and *S. orientale* were collected from two different populations occurring in contrasting environments. The northern area of La Laguna (mean annual precipitation = 526.9 mm; aridity index = 0.68) and the southern area of Vilaflor (mean annual precipitation = 396.3 mm; aridity index = 0.53) were the wetter collection sites for *H. incana* and *S. orientale* populations, respectively. The drier sites were the southern areas of Guímar (mean annual precipitation = 311.8 mm; aridity index = 0.39) and the region of Arico Bueno (mean annual precipitation = 264.3 mm; aridity index = 0.34), for *H. incana* and *S. orientale*, respectively (Supplementary Data Fig. S1).

The four annual species of Asteraceae, *Cladanthus mixtus* (L.) Oberpr. & Vogt., *Coleostephus myconis* (L.) Cass., *Glebionis coronaria* (L.) Cass ex Spach and *Glebionis segetum* (L.) Fourr. included in this study were investigated by Dória et al. (2018), during the spring of 2016 in Tenerife in the area of La Laguna (mean annual precipitation = 526.9 mm; aridity index = 0.68), following the same methodological procedures described below. For both the Brassicaceae and Asteraceae species, we harvested 10–20 individuals per species. All the species studied are annual herbaceous species, but some species (especially *S. alba* and *S. arvensis*) show a tendency to become biannual, which may be a consequence of the release of seasonality compared with the European mainland (Carlquist, 1974).

All individuals were collected from the soil, with roots still attached, quickly wrapped in wet tissues and sealed in plastic bags. Afterwards, the stems were stored in a cold room (around 5 °C) for a maximum of 5 d at the University of La Laguna, Tenerife. The sealed plastic bags were shipped by plane and immediately stored in a fridge for a maximum of 2 weeks at the caviplace facility to perform the hydraulic measurements (University of Bordeaux, France).

#### Xylem vulnerability to embolism

One to three stems per individual from at least ten individuals per species were used to measure vulnerability to embolism. Prior to measurements, all the stems were cut under water in the lab with a razor blade into a standard length of 27 or 42 cm in order to fit the two cavitron rotors used, and we confirmed that the vessels were shorter than the stem segments using the air pressure technique at 0.2 MPa. The cavitron is a modified centrifuge allowing the negative pressure in

the central part of the stem segment to be lowered by spinning the stems at different speeds while simultaneously measuring the water transport in the vascular system (Cochard, 2002; Cochard et al., 2013). First, the maximum hydraulic conductance of the stem in its native state ( $K_{\max}$  in  $\text{m}^2 \text{MPa}^{-1} \text{s}^{-1}$ ) was calculated under xylem pressure close to zero MPa using a reference ionic solution of 10 mM KCl and 1 mM  $\text{CaCl}_2$  in deionized ultrapure water. The rotation speed of the centrifuge was then gradually increased by  $-0.5$  or  $-1$  MPa to lower xylem pressure. The percentage loss of conductivity (PLC) of the stem was determined at each pressure step following the equation:

$$\text{PLC} = 100 \left( 1 - \frac{K}{K_{\max}} \right) \quad (1)$$

where  $K_{\max}$  represents the maximum conductance of the stem and  $K$  represents the conductance associated at each pressure step.

The vulnerability curves, showing the change in percentage loss of conductivity according to the xylem pressure, were obtained using the Cavisoft software (Cavisoft v1.5, University of Bordeaux, Bordeaux, France). A sigmoid function (Pammenter and Van der Willigen, 1998) was fitted to the data from each sample, using the following equation with SAS 9.4 (SAS 9.4, SAS Institute, Cary, NC, USA):

$$\text{PLC} = \frac{100}{\left[ 1 + \exp \left( \frac{S}{25} * (P_i - P_{50}) \right) \right]} \quad (2)$$

where  $S$  (%  $\text{MPa}^{-1}$ ) is the slope of the vulnerability curve at the inflexion point,  $P$  is the xylem pressure value used at each step, and  $P_{50}$  is the xylem pressure inducing 50 % loss of hydraulic conductivity. The parameters  $S$  and  $P_{50}$  were averaged for each species.

#### Stem anatomy

Light microscopy (LM), scanning electron microscopy (SEM) and transmission electron microscopy (TEM) were performed at Naturalis Biodiversity Center, the Netherlands, based on the samples for which we had obtained suitable vulnerability curves. The samples were taken from three individuals per species for LM and SEM, and from two individuals per species for TEM, from the middle part of the stem, where the negative pressure caused embolism formation during the cavitron experiment. The lab protocols for LM, SEM and TEM followed Dória et al. (2018). All the anatomical measurements were done using ImageJ (National Institutes of Health, Bethesda, MD, USA), largely following the suggestions of Scholz et al. (2013) and the IAWA Committee (1989).

Amongst the anatomical characters measured using LM, several indicators for lignification were calculated using a cross-section, such as the proportion of lignified area per total stem area [ $P_{\text{LIG}}$ , measuring the sum of primary xylem area, secondary xylem (= wood) area and fibre caps area in the cortex and dividing it by the total stem area], the proportion of xylem fibre wall area per fibre area ( $P_{\text{FW}}F_x$ , at the level of a single cell), and the thickness-to-span ratio of vessels ( $T_wD_v$ ). The diameter



of vessels ( $D_v$ ) was calculated based on the lumen area that was considered to be a circle according to the equation:

$$D_v = \sqrt{\frac{4A}{\pi}} \quad (3)$$

where  $D_v$  is the vessel diameter and  $A$  is the vessel lumen area. The hydraulically weighted vessel diameter ( $D_H$ ) was calculated following the equation:

$$D_H = \frac{\sum D_v^5}{\sum D_v^4} \quad (4)$$

where  $D_v$  is the vessel diameter as measured in eqn (3).

The ultrastructure of intervessel pits was observed using a field emission scanning electron microscope (Jeol JSM-7600F, Tokyo, Japan) and a JEOL JEM 1400-Plus transmission electron microscope (JEOL, Tokyo, Japan), as described in Dória *et al.* (2018). Since we observed intervessel pit membranes from the central stem segment parts where centrifugal force was applied, our measurements provide a relative estimation of intervessel pit membrane thickness.

### Statistical analyses

We tested the effect of both species and mean annual precipitation on the various hydraulic parameters ( $P_{12}$ ,  $P_{50}$ ,  $P_{88}$  and slope) using an analysis of covariance (ANCOVA). A log transformation, when necessary, was applied to the predictive variables to deal with heteroscedasticity and/or non-normality (Zuur *et al.*, 2007). A post-hoc Tukey's HSD test, from the R package Agricolae (Mendiburu, 2017), was used to test whether hydraulic parameters differ amongst species. To test the difference in  $P_{50}$  between the two Brassicaceae populations growing in contrasting environments (*H. incana* and *S. orientale*), we used linear mixed effects model, with the factor species as random effect, from the nlme R package (Pinheiro *et al.*, 2018).

We applied simple linear regressions to test for the relationship between  $P_{50}$ , climate data and anatomical variables. A log transformation, when necessary, was performed on the predictive variables to deal with heteroscedasticity and/or non-normality (Zuur *et al.*, 2007).

In order to evaluate which anatomical variables explain embolism resistance, we performed a multiple linear regression with  $P_{50}$  as response variable and stem anatomical characters as predictive variables. We selected *a priori* the predictive variables using biological knowledge based on previously published studies in combination with a pairwise scatterplot to detect the presence of correlations and collinearities. Then, we conducted a variance inflation factor (VIF) analysis, keeping only variables with a VIF value <2 (Zuur *et al.*, 2010). Subsequently, we followed the model simplification removing each time the least significant variable, until all the remaining terms in the model were significant (Crawley, 2007). The regression or differences were considered significant if  $P < 0.05$ . Next, we calculated the hierarchical partitioning (Chevan and Sutherland, 1991) for the variables retained in the model in order to assess their relative importance to explain  $P_{50}$ .

Independent *t*-tests were used to compare stem anatomical differences between the two populations of Brassicaceae species collected in contrasting environments.

To test whether differences in mean annual precipitation for each sampling site ( $P_R$ ) explained the combined variation of  $P_{50}$  and the anatomical characters, including also these characters that were not retained in the multiple regression analysis (the proportion of xylem fibre wall area per fibre area as observed in a cross-section, the thickness-to-span ratio of vessels and the hydraulically weighted vessel diameter), we performed a permutational multivariate analysis of variance (PERMANOVA). The anatomical characters and  $P_{50}$  are the response variables (rank transformed) and the mean annual precipitation is the predictive variable. PERMANOVA was performed using the adonis function in the Vegan R package (Oksanen *et al.*, 2015), based on Euclidean distances and 999 permutations. Later, a principal component analysis (PCA) was conducted using the function rda in the package Vegan, to observe simultaneously the relationships amongst the species, the main stem anatomical variables, the physiological variable ( $P_{50}$ ) and the mean annual precipitation ( $P_R$ ). We tested the relationship between some of the stem anatomical variables used in PCA with Pearson's coefficient correlation.

All analyses were performed using R version 3.4.3 (R Core Team, 2017) in R Studio version 1.1.414 (R Studio Team, 2016). All the differences were considered significant when  $P$  was <0.05.

## RESULTS

### Interspecific and intraspecific vulnerability to xylem embolism in the herbaceous stems

The 11 herbaceous species studied show stem  $P_{50}$  values varying 2-fold from −2.1 MPa to −4.9 MPa (Figs 1 and 2A; see Dória *et al.*, 2018 for the vulnerability curves of Asteraceae species) (Supplementary Data Table S1). The range of stem  $P_{50}$  shows significant interspecific variation ( $F = 27.161$ ,  $P < 0.001$ ; Fig. 2A), with no interaction between species and mean annual precipitation ( $F = 2.948$ ,  $P = 0.0901$ ) (Supplementary Data

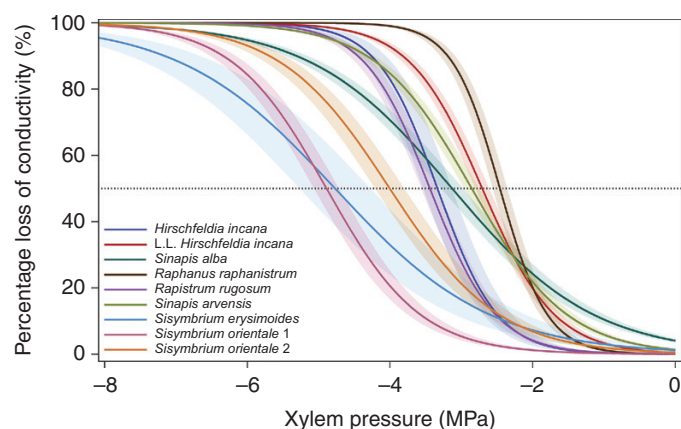


FIG. 1. Mean vulnerability curves for each of the seven herbaceous Brassicaceae species studied native to different vegetation zones of Tenerife (Canary Islands), with reference to the sampling localities for *Hirschfeldia incana* and *Sisymbrium orientale*. Shaded bands represent  $P_{50}$  standard errors, and 50 % percentage loss of conductivity (PLC) is indicated by the horizontal dotted line. L.L. refers to the more humid population of *H. incana* collected in the city of La Laguna. The numbers 1 and 2 of *Sisymbrium orientale* refer to the populations collected in drier and more humid sites, respectively. See Supplementary Data Fig S1.

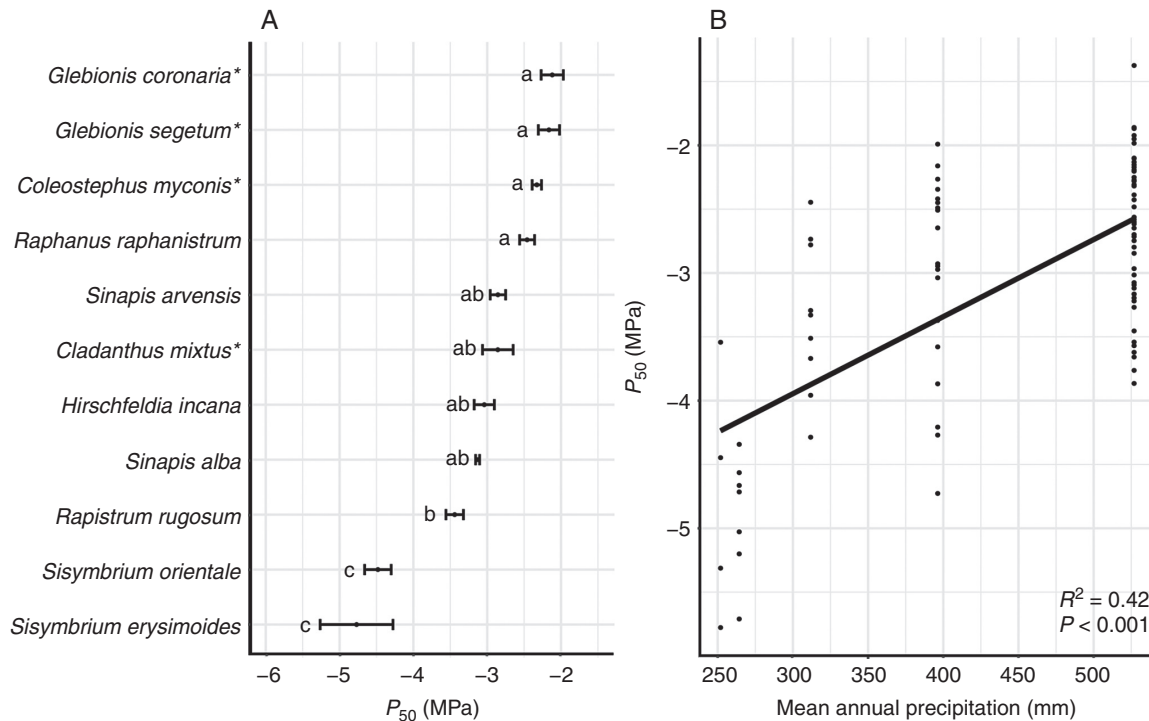


FIG. 2. Range of stem  $P_{50}$  amongst seven herbaceous Brassicaceae and four Asteraceae (represented with an asterisk; data from Dória *et al.*, 2018) species from different vegetation zones in Tenerife (Canary Islands, Spain), and its relationship to mean annual precipitation. (A) Mean values of stem  $P_{50}$  of the herbaceous Brassicaceae and Asteraceae species studied. Standard errors are represented by bars. Different letters indicate differences between species at  $P < 0.05$ . (B) Relationship between  $P_{50}$  and mean annual precipitation at the individual level (on average six individuals per species). The adjusted  $R^2$  and level of significance is given.

Table S3). Species explain 70 % of the variance, regardless of the variation in mean annual precipitation for the sampling sites, while the mean annual precipitation ( $P_R$ ) explains 30 % of the variance, regardless of the variation in species ( $F = 16.689$ ,  $P < 0.001$ ; Fig. 2B) (Supplementary Data Table S3). Likewise, significant interspecific variations are also observed for  $P_{88}$  and  $P_{12}$  ( $F = 22.507$ ,  $P < 0.001$ ;  $F = 7.868$ ,  $P < 0.001$ , respectively) with part of both variations explained by  $P_R$  ( $F = 6.506$ ,  $P < 0.05$ ;  $F = 4.439$ ,  $P < 0.05$  for  $P_{88}$  and  $P_{12}$ , respectively). Variation in slope amongst the species studied is also significant ( $F = 4.940$ ,  $P < 0.001$ ), but the mean precipitation is not significant for this parameter ( $F = 0.138$ ,  $P = 0.712$ ).

The two Brassicaceae populations of *H. incana* and *S. orientale* show significant intraspecific variation in  $P_{50}$  ( $P < 0.001$ ,  $F = 17.6083$ ), demonstrating that the contrasting environments are important to explain the intraspecific variation in  $P_{50}$  (Fig. 3). For *H. incana*, the drier site receives on average 311.8 mm of mean annual precipitation (aridity index = 0.39), while the more humid site receives on average 526.9 mm (aridity index = 0.68). For *S. orientale*, the drier site has on average 264.3 mm of mean annual precipitation, and the more humid site 396.3 mm for the same period (aridity index = 0.34 and 0.53, respectively) (Supplementary Data Fig. S1).

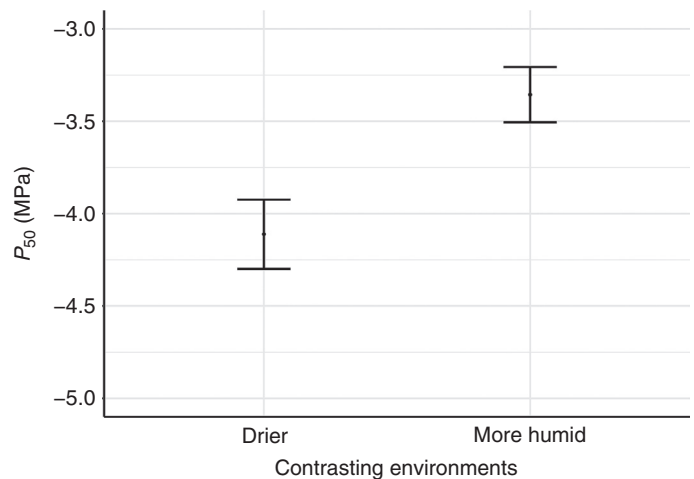


FIG. 3. Intraspecific differences of mean stem  $P_{50}$  between the two populations of the Brassicaceae, *Hirschfeldia incana* and *Sisymbrium orientale*, collected in contrasting environments (*H. incana*: mean annual precipitation = 311.8 mm; aridity index = 0.39 for the drier site, and mean annual precipitation = 526.9 mm; aridity index = 0.68 for the more humid site. *S. orientale*: mean precipitation = 264.3 mm; aridity index = 0.34 for the drier site, and mean annual precipitation = 396.3 mm; aridity index = 0.53 for the more humid site.)

Structure–function relationships in the herbaceous stems show correlation between embolism resistance and anatomy

The stem anatomical variables that best explain the variation in  $P_{50}$  are the proportion of lignified area per total stem area ( $P_{LIG}$ ;

which is a measure of stem woodiness) (Fig. 4) and the thickness of the intervessel pit membrane ( $T_{PM}$ ) (Fig. 5) ( $P < 0.001$ ;  $R^2 = 0.6783$ ) (Supplementary Data Tables S2 and S4). The  $P_{50}$ – $P_{LIG}$  relationship remains significant for the separate data sets ( $P < 0.001$ ;  $R^2 = 0.58$  for Brassicaceae and  $P < 0.01$ ;  $R^2 = 0.48$

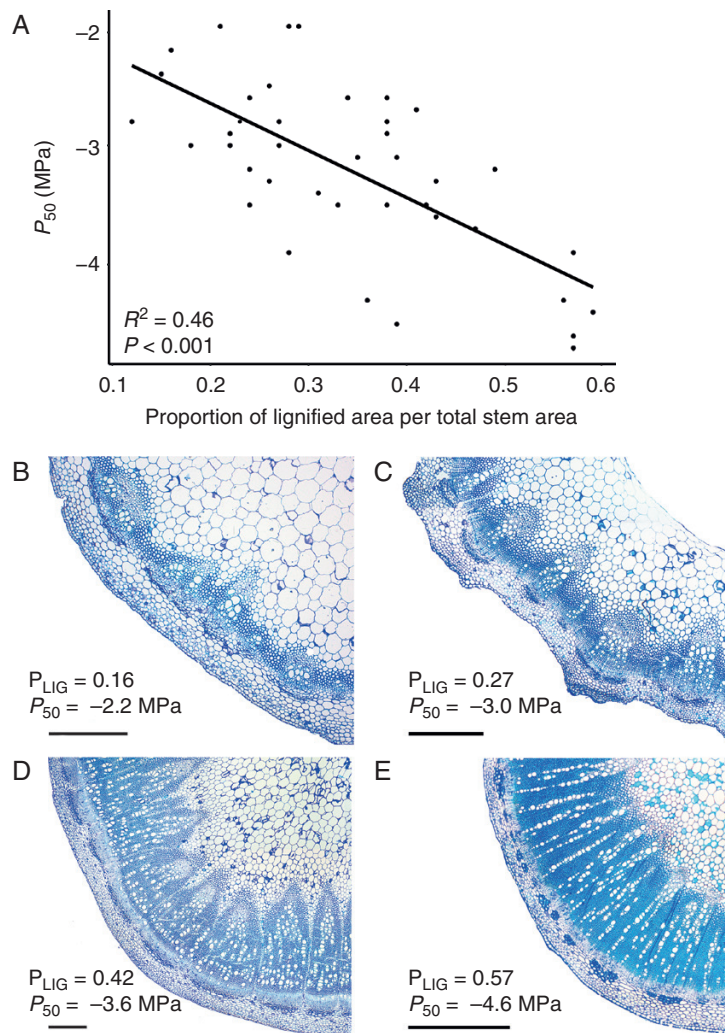


FIG. 4. Relationships between stem  $P_{50}$  and the proportion of lignified area per total stem area ( $P_{LIG}$ ). (A) Linear regression between  $P_{50}$  and  $P_{LIG}$ . The adjusted  $R^2$  and the level of significance are given. Each dot represents one individual (on average three individuals per species). (B–E) Light microscope images of cross-sections through the stem of Brassicaceae species showing an increase of  $P_{LIG}$  matching with an increase in embolism resistance. (B) *Raphanus raphanistrum*. (C) *Sinapis alba*. (D) *Rapistrum rugosum*. (E) *Sisymbrium orientale* from the drier sampling site. The scale bars represent 500  $\mu$ m.

for Asteraceae), while the  $P_{50}$ – $T_{PM}$  correlation disappears when analysing the Brassicaceae and Asteraceae data sets separately ( $P = 0.2164$ ,  $R^2 = 0.040$  vs.  $P = 0.6175$ ,  $R^2 = -0.099$ , respectively). In addition,  $P_{LIG}$  is the main variable explaining 69 % of the  $P_{50}$  variation, while  $T_{PM}$  explains the remaining 31 % (Supplementary Data Tables S4).

The *S. orientale* population growing in the drier sampling site shows a higher proportion of lignified area per total stem area ( $P_{LIG}$ ), thicker intervessel pit membranes ( $T_{PM}$ ) and thicker intervessel walls ( $T_{VW}$ ) than the population growing in the more humid sampling site (Fig. 6; Table 1) (Supplementary Data Table S2). No significant anatomical differences were found between the two populations of *H. incana* growing in contrasting environments.

All Brassicaceae observed have vested pits (Fig. 5B–D and 6C, D), while these are absent in the Asteraceae species. No differences in the level of vesturing are observed amongst the embolism-resistant vs. vulnerable Brassicaceae species.

#### Relationship between mean precipitation ( $P_R$ ), stem anatomy and $P_{50}$

The PERMANOVA test shows that the mean annual precipitation explains the variation in both stem anatomical characters and  $P_{50}$  ( $F = 3.8098$ ,  $R^2 = 0.14$ ,  $P < 0.05$ ) (Supplementary Data Table S5).

When analysing the association amongst stem anatomical characters, mean annual precipitation and  $P_{50}$  using a PCA, the first axis of the PCA explains 40 % of the total variance observed, while the second axis explains 21 %. The first principal component has large positive associations with  $P_{50}$ , and with mean annual precipitation ( $P_R$ ), and negative associations with the proportion of lignified area per total stem area as observed in a cross-section ( $P_{LIG}$ ), the proportion of xylem fibre wall area per fibre area as observed in a cross-section ( $P_{FW}^{FX}$ ) and the thickness of intervessel pit membranes ( $T_{PM}$ ) (Fig. 7). Along this first axis, the proportion of xylem fibre wall per fibre is correlated with  $P_{50}$  ( $P < 0.01$ ,  $r = -0.45$ ). The second



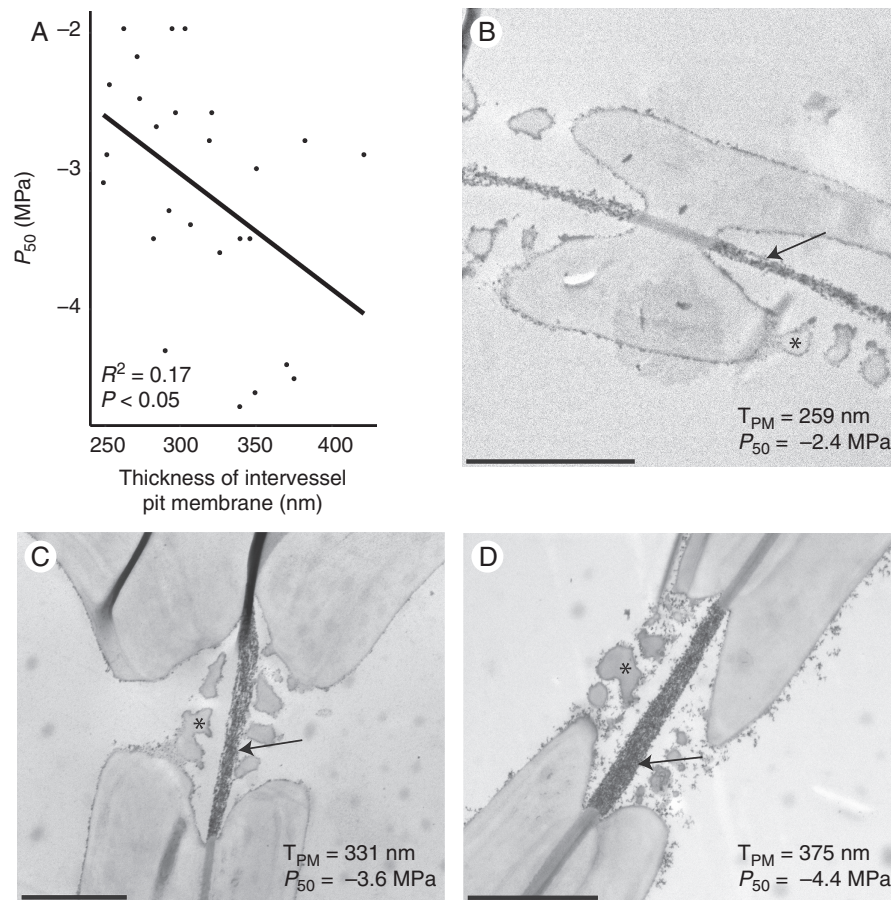


FIG. 5. Relationships between stem  $P_{50}$  and thickness of the intervessel pit membrane ( $T_{PM}$ ). (A) Linear regression between  $P_{50}$  and  $T_{PM}$ . The adjusted  $R^2$  and the level of significance are given. Each dot represents one individual (on average two individuals per species). (B–D) Transmission electron microscope images of intervessel pits of Brassicaceae species showing thicker pit membranes (arrows) in species that are more embolism resistant; all the herbaceous Brassicaceae species studied have vestures (asterisks). (B) *Raphanus raphanistrum*. (C) *Rapistrum rugosum*. (D) *Sisymbrium erysimoides*. Scale bars represent 2  $\mu$ m.

principal component has a large positive association with the hydraulically weighted vessel diameter ( $D_H$ ) and a negative association with the thickness-to-span ratio of vessels ( $T_w D_v$ ). These two variables are negatively correlated with each other ( $P < 0.01$ ,  $r = -0.51$ ), but neither of them is correlated with embolism resistance ( $P = 0.7608$ ,  $r = -0.0525$ ;  $P = 0.5662$ ,  $r = -0.0988$ ). The thickness of the vessel is also not correlated with  $T_w D_v$  ( $P = 0.2811$ ,  $r = 0.1846$ ). The individuals distributed at the right side of the multivariate PCA space are associated with less negative values of  $P_{50}$  and higher mean annual precipitation. Some of these individuals present higher values of the thickness-to-span ratio of vessels, while others have higher hydraulically weighted vessel diameters. In contrast, the individuals at the left side of the multivariate PCA space are associated with more negative values of  $P_{50}$ , more pronounced lignification characters, thicker intervessel pit membranes and lower mean annual precipitation (Fig. 7).

Individuals of the two Brassicaceae populations of *H. incana* (represented by circles) and *S. orientale* (represented by triangles) occupy different areas of the multivariate space (Fig. 7). The individuals collected in drier sites (open circles for *H. incana* and open triangles for *S. orientale*) are associated with a higher degree of lignification characters, thicker intervessel pit membranes and lower values of mean annual

precipitation (Fig. 7). The individuals collected in more humid sites (filled circles for *H. incana* and filled triangles for *S. orientale*) are associated with higher hydraulically weighted vessel diameter and higher values of the thickness-to-span ratio of vessels (Fig. 7).

## DISCUSSION

### *Interspecific and intraspecific stem $P_{50}$ variation across herbaceous eudicots is strongly linked to precipitation*

Our data set, comprising 11 herbaceous species of Brassicaceae and Asteraceae from five different habitats in Tenerife with a mean annual precipitation from 252 to 527 mm, shows a 2-fold range of stem  $P_{50}$  values that match the precipitation values of the sampling sites: the most vulnerable species ( $P_{50} -2.1$  MPa) was collected from wetter environments and the most resistant species ( $P_{50} -4.9$  MPa) was sampled from drier vegetation types (Figs 1 and 2). The explanatory power of mean annual precipitation towards stem  $P_{50}$  supports the functional relevance of resistance to xylem embolism as an adaptive response to water deficit, as has been repeatedly demonstrated for woody trees (Maherali et al., 2004; Blackman et al., 2012; Choat et al., 2012) and to a lesser extent also herbs (mainly

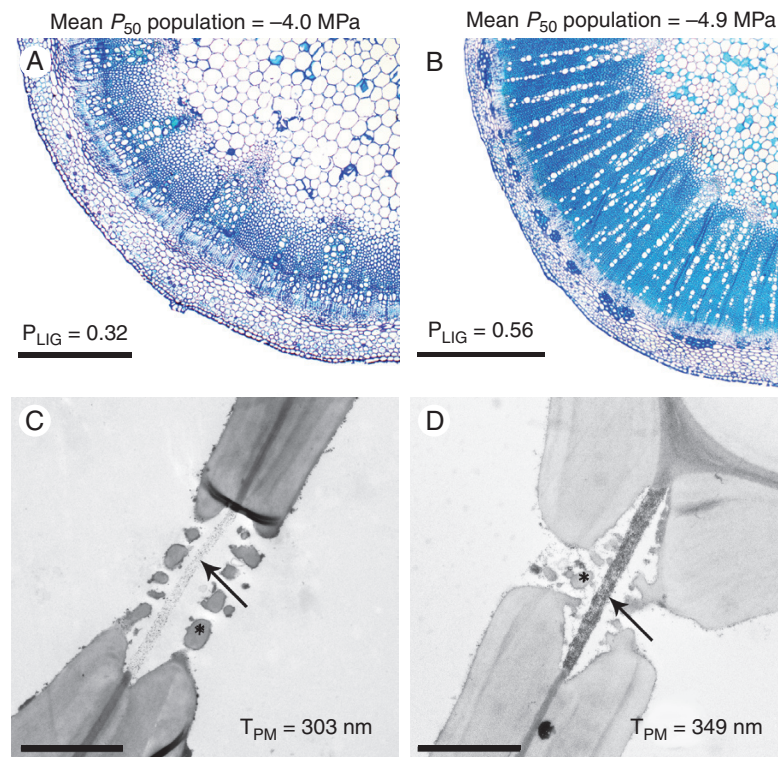


FIG. 6. Intraspecific differences between two populations of *Sisymbrium orientale* growing in the more humid habitat (A, C) vs. the drier sampling site (B, D). (A, B) Light microscope image of cross-sections through the stems showing the population mean  $P_{50}$  values and proportion of lignified area per total stem area ( $P_{LIG}$ ). Scale bars represent 500  $\mu\text{m}$ . (C, D) Transmission electron microscope images of intervessel pits showing the population mean of thickness of the intervessel pit membrane ( $T_{PM}$ ) (arrows). Vestures are marked with an asterisk. Scale bars represent 2  $\mu\text{m}$ .

TABLE 1. Stem anatomical variables that showed significant t-test differences between the two populations of *Sisymbrium orientale* growing in contrasting environments

Stem anatomical variable	Mean for <i>S. orientale</i> from the drier site	Mean for <i>S. orientale</i> from the more humid site	t-test (P-value)
Proportion of lignified area per total stem area	0.57	0.32	0.00763
Thickness of intervessel pit membrane (nm)	349.14	303.43	0.04231
Thickness of intervessel wall ( $\mu\text{m}$ )	3.70	3.31	0.01194

Mean annual precipitation for the drier site is 264.3 mm and for the more humid site is 396.3 mm; the aridity indexes are 0.34 and 0.53, respectively.

grasses, [Lens et al., 2016](#)). Likewise, the intraspecific (between-population) differences in stem  $P_{50}$  for both *S. orientale* and *H. incana* ([Fig. 3](#)) are also explained by mean annual precipitation: for both species, the more embolism-resistant populations occur in areas with less annual precipitation. This suggests that differences in habitat amongst herbaceous populations from the same species can increase the intraspecific plasticity in  $P_{50}$ .

Percentage of lignified area per total stem area ( $P_{LIG}$ ) outcompetes intervessel pit membrane ( $T_{PM}$ ) as the explanatory variable explaining variation in stem  $P_{50}$

The percentage of lignified area per total stem area ( $P_{LIG}$ ), which is mainly defined by the amount of woodiness in the herbaceous stems as observed in a cross-section, is the character that best explains the variation of embolism resistance in stems, with more lignified stems being more resistant to embolism

([Fig. 4](#)). Since the germination time of the herbaceous species on Tenerife does more or less converge after the arrival of the rains in autumn and winter, we believe that the differences in woodiness is species and/or niche specific rather than dependent on major differences in stem age between species. For example, the three species (*Raphanus raphanistrum*, *Sinapis arvensis* and the population of *Sisymbrium orientale* from the more humid area) collected in Vilaflor village (sampling site 4 of [Supplementary Data Fig. S1](#)) show a 2-fold difference in the degree of woodiness matching nicely with stem  $P_{50}$ , despite the fact that these three populations occurred along the same road ([Supplementary Data Tables S1 and S2](#)). The relationship between characters related to higher stem lignification and higher absolute values of  $P_{50}$  has been recorded for different plant groups, both in woody ([Hacke et al., 2001](#); [Jacobsen et al., 2005](#); [Jansen et al., 2009](#); [Pereira et al., 2017](#)) and in herbaceous lineages ([Lens et al., 2012b, 2013, 2016](#); [Tixier et al., 2013](#)) and in closely related woody lineages that are derived



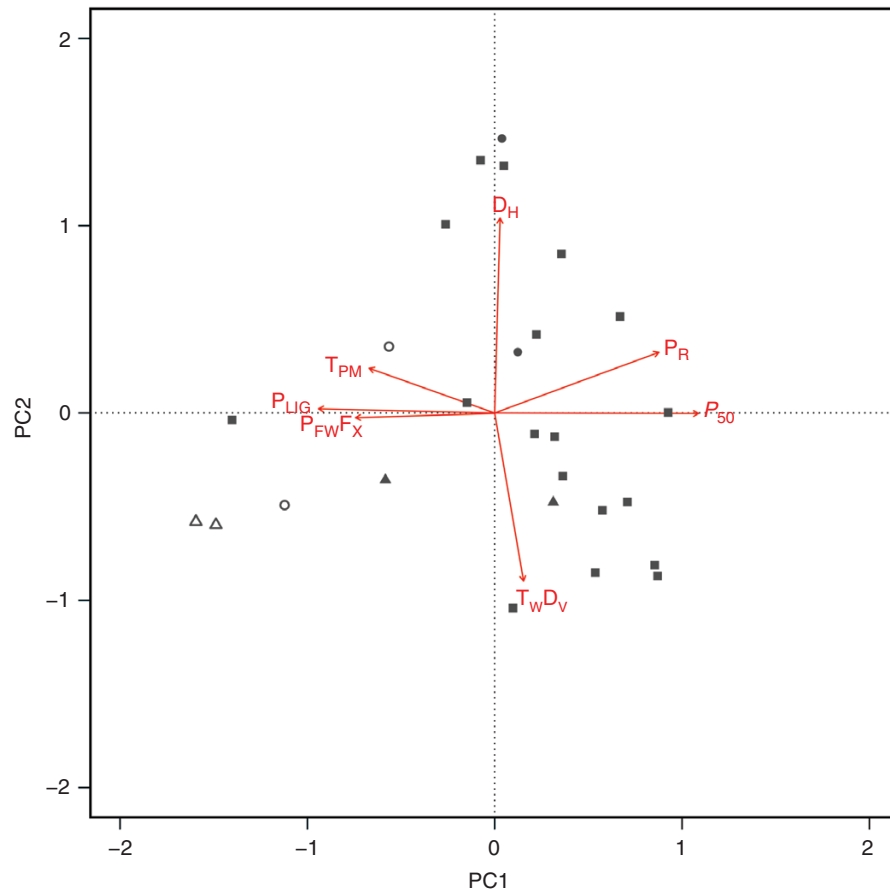


FIG. 7. Principal component analysis of stem anatomical characters, mean annual precipitation and  $P_{50}$  on the first two axes.  $P_{LIG}$  = proportion of lignified area per total stem area as observed in a cross-section;  $P_{FWFX}$  = proportion of xylem fibre wall area per fibre area as observed in a cross-section;  $P_R$  = mean annual precipitation;  $T_WDV$  = thickness-to-span ratio of vessels;  $P_{50}$  = pressure inducing 50 % loss of hydraulic conductivity;  $D_H$  = hydraulically weighted vessel diameter;  $T_{PM}$  = thickness of intervessel pit membrane. Circles represent individuals of *H. incana* from humid (filled) and dry (open) sampling sites, while triangles refer to individuals of *S. orientale* from the humid (filled) and dry (open) sites. The squares represent the other individuals of Brassicaceae and Asteraceae studied.

from herbaceous relatives (Dória et al., 2018). Differences in the proportion of the lignified area in the stem are also found at the intraspecific level in this study, with the more resistant population of *S. orientale* showing thicker intervessel walls and higher  $P_{LIG}$  values compared with those of the more vulnerable population (Fig. 6; Table 1). The higher  $P_{LIG}$  values in the drier population could also be strengthened by the presumably earlier germination time in the area of El Escobonal (470 m asl), which is about 900 m lower than the colder (and wetter) site of Vilaflor (1400 m asl), making the stems of the drier (and lower) site older, enabling them to lignify more.

It is challenging to relate increased stem lignification functionally with embolism resistance, since most lignification characters do not directly influence embolism formation and spread in the 3-D network of angiosperm vessels. Indeed, the thickness of intervessel pit membranes ( $T_{PM}$ ) is more likely to affect the length of the tortuous and irregularly shaped pores that air–water menisci need to cross before air–seeding may occur, explaining the spread of embolism through intervessel pit membranes into adjacent conduits (Jansen et al., 2009; Lens et al., 2011, 2013; Li et al., 2016). Although the  $P_{50}$ – $T_{PM}$  relationship is confirmed in our herbaceous eudicot data set (Fig. 5),  $T_{PM}$  provides a much lower power to explain differences in  $P_{50}$  compared with the

degree of woodiness as observed in a cross-section, calculated as the percentage of lignified area per total stem area ( $P_{LIG}$ ). This may seem surprising, but studies investigating the relationship between stem  $P_{50}$  and  $T_{PM}$  amongst herbaceous species are scarce and the functional relevance of  $T_{PM}$  in herbs might be less important compared with woody species. A few examples that suggest this poor  $P_{50}$ – $T_{PM}$  relationship in herbs are: the  $P_{50}$ – $T_{PM}$  relationship disappears in our study when only including the Brassicaceae species; no link between  $P_{50}$  and  $T_{PM}$  was found in a grass data set based on four species with contrasting  $P_{50}$  values (Lens et al., 2016); and a third study investigating closely related herbaceous and woody daisies showed that the  $P_{50}$ – $T_{PM}$  relationship was retrieved only when the herbaceous data set was combined with the woody data set (Dória et al., 2018). Evidently, more work on stem  $P_{50}$  and additional anatomical measurements based on the same – properly fixated – herbaceous stems is needed to shed more light on the functional relevance of  $T_{PM}$  in herbs, which should in theory match the hydraulic importance of  $T_{PM}$  as observed in shrubs and trees (Li et al., 2016).

Relationships between increased lignification and thicker intervessel pit membranes have been reported, which could explain the indirect correlation between higher lignification and

higher embolism resistance (Jansen *et al.*, 2009; Li *et al.*, 2016; Dória *et al.* 2018). These findings are in accordance with our results for the two populations of *S. orientale* collected in contrasting environments (Table 1; Fig. 6): the more resistant population shows a higher proportion of lignified area in the stem, thicker intervessel wall, and thicker intervessel pit membranes. However, the  $T_{PM}$ –lignification correlation disappears in our entire data set (including Asteraceae and Brassicaceae species), showing that increased lignification characters are not necessarily linked to thicker intervessel pit membranes.

*The mean precipitation explains both  $P_{50}$  and anatomical variation in stems of herbaceous eudicots*

Mean annual precipitation explains both the variation in stem  $P_{50}$  and the variation in stem anatomical characters across the herbaceous species studied. It has been well documented that environmental factors influence  $P_{50}$  (Maherali *et al.*, 2004; Choat *et al.*, 2012; Trueba *et al.*, 2017) as well as anatomical traits (Carlquist, 1975; Baas *et al.*, 1983; Lens *et al.*, 2004; Dória *et al.*, 2016; O'Brien *et al.*, 2017). In our study, populations from drier sites show stems with more negative  $P_{50}$  values and more pronounced lignification, such as the proportion of lignified area per total stem area (a measure of the amount of woodiness) and the proportion of xylem fibre wall area per fibre area as observed in a cross-section. These characters are most associated with the first PCA axis (Fig. 7).

Our results show that the common pattern observed for woody species, i.e. a shift in rainfall patterns associated with survival and distribution of trees and shrubs (Engelbrecht *et al.*, 2007; Allen *et al.*, 2010; Trueba *et al.*, 2017), and drought-induced tree mortality associated with substantial loss of hydraulic conductivity across taxa and biomes (Adams *et al.*, 2017), is also true for herbaceous species (see also the first section of the Discussion). At the same time, different environment conditions also impact stem anatomical characters allowing plants to adapt to changing climates (Carlquist, 1975; Baas *et al.*, 1983; Martínez-Vilalta *et al.*, 2010; Kattge *et al.*, 2011).

Across woody trees, a lineage-specific sub-set of stem anatomical traits can be linked to drought-induced embolism resistance, such as increased wood density (linked to fibre wall thickness in angiosperms; Chave *et al.*, 2009; Zieminska *et al.*, 2013), increased thickness-to-span ratio of conduits (Hacke *et al.*, 2001; Bouche *et al.*, 2014), thicker intervessel pit membranes (Jansen *et al.*, 2009; Lens *et al.*, 2011; Li *et al.*, 2016; Dória *et al.*, 2018) and narrower vessel diameters (Poorter *et al.*, 2010; Hacke *et al.*, 2016; Olson *et al.*, 2018). Amongst herbaceous species, fragile stems also need to be reinforced by a suite of mechanical characters, as shown in our study: individuals occurring in drier areas show a higher degree of lignification/woodiness ( $P_{LIG}$ ) and thicker intervessel pit membranes (Fig. 7) (see previous section). The increment of cellular support against implosion is often cited as the reason for this hydraulic–mechanical trade-off, which can result from either an increase in vessel wall to lumen ratio (Hacke *et al.*, 2001; Jacobsen *et al.*, 2007; Cardoso *et al.*, 2018) or an increase in fibre matrix support (more and thicker walled xylem fibres) (Jacobsen *et al.*, 2005, 2007; Pratt and Jacobsen, 2017; Dória *et al.*, 2018). For the herbaceous species studied here, we found

the latter relationship, demonstrated by the correlation between a higher proportion of xylem fibre cell wall per fibre ( $P_{FW}F_X$ ) and more negative  $P_{50}$ . Both kinds of cellular reinforcements, due to either vessel wall reinforcements or a more pronounced surrounding fibre matrix, would result in increasing xylem density offering support against implosion. In accordance with this hydraulic–mechanical trade-off, collapse of xylem conduits was only observed in cells that lack a robust support of the fibre matrix, for instance in leaves (Cochard *et al.*, 2004; Brodribb and Holbrook, 2005; Zhang *et al.*, 2016) and in low-lignin stems of poplar mutants (Kitin *et al.*, 2010). Our study confirms that increasing the mechanical strength of fragile herbaceous stems using a suite of lignification characters may be highly relevant to acquire a higher level of embolism resistance.

Another aspect of the hydraulic–mechanical relationship in our data set is highlighted by the negative correlation between the thickness-to-span ratio of vessels ( $T_wD_v$ ), determining the resistance to implosion of the conduit, and the hydraulically weighted vessel diameter ( $D_H$ ). Since there is a significant relationship between  $T_wD_v$  and  $D_H$ , but not between  $T_wD_v$  and the thickness of the vessel wall ( $T_{vw}$ ), it can be concluded that vessel diameter impacts much more the variation of  $T_wD_v$  than the thickness of vessel wall. It is known that larger vessel lumina increase hydraulic conductivity (Tyree and Zimmerman, 2002) and, because in our data set vessel wall thickness remains more or less the same, it gives rise to larger vessels that become mechanically weaker and potentially more vulnerable (Preston *et al.*, 2006; Zanne *et al.*, 2010; Pratt and Jacobsen, 2017). However, in our data set,  $P_{50}$  is not correlated with  $D_H$ , with  $T_{vw}$  or with  $T_wD_v$ , meaning that the vessel diameter and thickness-to-span ratio of vessels do not impact embolism resistance in our herbaceous data set.

In conclusion, this study investigated structure–function relationships in stems of seven herbaceous Brassicaceae occurring in different vegetation zones across the island of Tenerife and merged the data set produced with a similar data set for herbaceous Asteraceae growing on the same island. The 2-fold difference in embolism resistance found here shows that stems of herbaceous eudicots are able to deal with a range of negative pressures inside xylem conduits, although the  $P_{50}$  range in woody trees remains considerably higher. In addition, mean annual precipitation is the major determinant influencing both embolism resistance and anatomical characters in the herbaceous stems, demonstrating the predictive value of both characters with respect to survival and distribution of herbs along environmental gradients. This improves our understanding of the evolutionary and ecological significance of embolism resistance in non-woody species. Our results also show that the degree of woodiness ( $P_{LIG}$ ) outcompetes the thickness of intervessel pit membranes ( $T_{PM}$ ) as the most powerful character determining embolism resistance in stems of herbaceous eudicots studied. This may question the hydraulic relevance of  $T_{PM}$  in herbs, although many more observations on embolism resistance and anatomical observations on herbaceous plants need to be carried out before a final conclusion can be reached.

#### SUPPLEMENTARY DATA

Supplementary data are available online at <https://academic.oup.com/aob> and consist of the following. Figure S1: map of Tenerife with the five sampling sites, each corresponding to

unique aridity indices. Table S1: hydraulic parameters of the herbaceous Brassicaceae species studied. Table S2: stem anatomical measurements of the herbaceous Brassicaceae species studied, along with the aridity indices and values for mean annual precipitation. Table S3: analysis of covariance of species and mean precipitation explaining the variance in  $P_{50}$  of the herbaceous Brassicaceae and Asteraceae species studied. Table S4: multiple regression model of anatomical features explaining the variance in  $P_{50}$  of the herbaceous Brassicaceae and Asteraceae species studied. Table S5: permutational multivariate analysis of variance of mean annual precipitation explaining the variance in  $P_{50}$  and in the main stem anatomical characters of the herbaceous Brassicaceae and Asteraceae species studied.

### ACKNOWLEDGEMENTS

We thank the Cabildo de Tenerife (AFF 147/13 no. Sigma, 2013-00748; AFF 429/13 no. Sigma, 2013-02030; AFF 149/15 no. Sigma, 2015-00925; AFF 85/16 no. Sigma, 2016-00838) and Teide National Park (no. 152587, REUS 27257, 2013; no. 536556, REUS 83804, 2013; Res. no. 222/2015) for the collection permits, and the AEMET - Agencia Estatal de Meteorología, Spanish Government, for providing meteorological data. We also acknowledge the technical support of R. Langelaan, W. Star and G. Capdeville. This work was supported by the CNPq - Conselho Nacional de Desenvolvimento Científico e Tecnológico, Brazil (PROC. no. 206433/2014-0), the Alberta Mennega Stichting, the Cluster of Excellence COTE (ANR-10-LABX-45, within the DEFI project) and the programme 'Investments for the Future' (ANR-10-EQPX-16, XYLOFOREST) funded by the French National Agency for Research.

### LITERATURE CITED

- Adams HD, Zeppel MJB, Anderegg WRL, et al. 2017. A multi-species synthesis of physiological mechanisms in drought-induced tree mortality. *Nature, Ecology and Evolution* 1: 1285–1291.
- Ahmad HB, Lens F, Capdeville G, Burlett R, Lamarque LJ, Delzon S. 2017. Intraspecific variation in embolism resistance and stem anatomy across four sunflower (*Helianthus annuus* L.) accessions. *Physiologia Plantarum* 163: 59–72.
- Allen CD, Macalady AK, Chenchouni H, et al. 2010. A global overview of drought and heat-induced tree mortality reveals emerging climate change risks for forests. *Forest Ecology and Management* 259: 660–684.
- Anderegg WRL, Klein T, Bartlett M, et al. 2016. Meta-analysis reveals that hydraulic traits explain cross-species patterns of drought-induced tree mortality across the globe. *Proceedings of the National Academy of Sciences, USA* 113: 5024–5029.
- Baas P, Werker E, Fahn A. 1983. Some ecological trends in vessel characters. *IAWA Bulletin* 4: 141–159.
- Blackman CJ, Brodribb TJ, Jordan GJ. 2012. Leaf hydraulic vulnerability influences species' bioclimatic limits in a diverse group of woody angiosperms. *Oecologia* 168: 1–10.
- Bouche PF, Larter M, Domes JC, et al. 2014. A broad survey of xylem hydraulic safety and efficiency in conifers. *Journal of Experimental Botany* 65: 4419–4431.
- Brodersen CR, McElrone AJ, Choat B, Lee EF, Shackel KA, Matthews MA. 2013. *In vivo* visualizations of drought-induced embolism spread in *Vitis vinifera*. *Plant Physiology* 161: 1820–1829.
- Brodribb T, Holbrook NM. 2005. Water stress deforms tracheids peripheral to the leaf vein of a tropical conifer. *Plant Physiology* 173: 1139–1146.
- Brodribb TJ, Bowman D, Nichols S, Delzon S, Burlett R. 2010. Xylem function and growth rate interact to determine recovery rates after exposure to extreme water deficit. *New Phytologist* 188: 533–542.
- Cardoso AA, Brodribb TJ, Lucani CJ, DaMatta FM, McAdam SAM. 2018. Coordinated plasticity maintains hydraulic safety in sunflower leaves. *Plant, Cell & Environment* 41: 2567–2576.
- Carlquist S. 1974. Insular woodiness. In: Carlquist SJ, ed. *Island biology*. New York: Columbia University Press, 350–428.
- Carlquist S. 1975. *Ecological strategies of xylem evolution*. Berkeley, CA: University of California Press.
- Challinor AJ, Ewert F, Arnold S, Simelton E, Fraser E. 2009. Crops and climate change: progress, trends, and challenges in simulating impacts and informing adaptation. *Journal of Experimental Botany* 60: 2775–2789.
- Chave J, Coomes D, Jansen S, Lewis SL, Swenson NG, Zanne AE. 2009. Towards a worldwide wood economics spectrum. *Ecology Letters* 12: 351–366.
- Chevan A, Sutherland M. 1991. Hierarchical partitioning. *American Statistical Association* 45: 90–96.
- Choat B, Sack L, Holbrook NM. 2007. Diversity of hydraulic traits in nine *Cordia* species growing in tropical forests with contrasting precipitation. *New Phytologist* 175: 686–698.
- Choat B, Jansen S, Brodribb TJ, et al. 2012. Global convergence in the vulnerability of forests to drought. *Nature* 491: 752–756.
- Cochard H. 2002. A technique for measuring xylem hydraulic conductance under high negative pressures. *Plant, Cell & Environment* 25: 815–819.
- Cochard H, Nardini A, Coll L. 2004. Hydraulic architecture of the leaf blades: where is the main resistance? *Plant, Cell & Environment* 27: 1257–1267.
- Cochard H, Herbette S, Barigah T, Badel E, Ennajeh M, Vilagrosa A. 2010. Does sample length influence the shape of xylem embolism vulnerability curves? A test with the Cavitron spinning technique. *Plant, Cell & Environment* 33: 1543–1552.
- Cochard H, Badel E, Herbette S, Delzon S, Choat B, Jansen S. 2013. Methods for measuring plant vulnerability to cavitation: a critical review. *Journal of Experimental Botany* 64: 4779–4791.
- Corcuera L, Cochard H, Gil-Pelegrin E, Notivol E. 2011. Phenotypic plasticity in mesic populations of *Pinus pinaster* improves resistance to xylem embolism ( $P_{50}$ ) under severe drought. *Trees* 25: 1033–1042.
- Crawley MJ. 2007. *The R book*. Chichester, UK: John Wiley & Sons Ltd.
- Dai AG. 2013. Increasing drought under global warming in observations and models. *Nature Climate Change* 3: 52–58.
- Davis SD, Sperry JS, Hacke UG. 1999. The relationship between xylem conduit diameter and cavitation caused by freezing. *American Journal of Botany* 86: 1367–1372.
- del-Arco M, Pérez-de-Paz PL, Acebes JR, et al. 2006. Bioclimatology and climatophilous vegetation of Tenerife (Canary Islands). *Annales Botanici Fennici* 43: 167–192.
- Dória LC, Podadera DS, Batalha MA, Lima RS, Marcatti RM. 2016. Do woody plants of the Caatinga show a higher degree of xeromorphism than in the Cerrado? *Flora* 224: 244–251.
- Dória LC, Podadera DS, del Arco M, et al. 2018. Insular woody daisies (*Argyranthemum*, Asteraceae) are more resistant to drought-induced hydraulic failure than their herbaceous relatives. *Functional Ecology* 32: 1467–1478.
- Dulin MW, Kirchoff BK. 2010. Paedomorphosis, secondary woodiness and insular woodiness in plants. *Botanical Review* 76: 405–490.
- Engelbrecht BMJ, Comita LS, Condit R, et al. 2007. Drought sensitivity shapes species distribution patterns in tropical forests. *Nature* 447: 80–82.
- Gleason SM, Westoby M, Jansen S, et al. 2016. Weak tradeoff between xylem safety and xylem-specific hydraulic efficiency across the world's woody plant species. *New Phytologist* 209: 123–136.
- Hacke UG, Sperry JS, Pockman WT, Davis SD, McCulloh KA. 2001. Trends in wood density and structure are linked to prevention of xylem implosion by negative pressure. *Oecologia* 126: 457–461.
- Hacke UG, Jansen S. 2009. Embolism resistance of three boreal conifer species varies with pit structure. *New Phytologist* 182: 675–686.
- Hacke UG, Spice R, Schreiber SG, Plavcova L. 2016. An ecophysiological and developmental perspective on variation in vessel diameter. *Plant, Cell & Environment* 40: 831–845.
- Hoffman WA, Marchin RM, Abit P, Lau LO. 2011. Hydraulic failure and tree dieback are associated with high wood density in a temperate forest under extreme drought. *Global Change Biology* 17: 2731–2742.
- Holste EK, Jerke MJ, Matzner SL. 2006. Long-term acclimatization of hydraulic properties, xylem conduit size, wall strength and cavitation



- resistance in *Phaseolus vulgaris* in response to different environmental effects. *Plant, Cell & Environment* **29**: 836–843.
- IAWA Committee. 1989. IAWA list of microscopic features for hardwood identification. *IAWA Bulletin* **10**: 219–332.
- Jacobsen AL, Ewers FW, Pratt RB, Paddock WA, Davis D. 2005. Do xylem fibers affect vessel cavitation resistance? *Plant Physiology* **139**: 546–556.
- Jacobsen AL, Pratt RB, Ewers FW, Davis SD. 2007. Cavitation resistance among 26 chaparral species of Southern California. *Ecological Monographs* **77**: 99–115.
- Jacobsen AL, Pratt RB, Tobin MF, Hacke UG, Ewers FW. 2012. A global analysis of xylem vessel length in woody plants. *American Journal of Botany* **99**: 1583–1591.
- Jansen S, Choat B, Pletsers A. 2009. Morphological variation of intervessel pit membranes and implications to xylem function in angiosperms. *American Journal of Botany* **96**: 409–419.
- Kattge J, Diaz S, Lavorel S, et al. 2011. TRY – a global database of plant traits. *Global Change Biology* **17**: 2905–2935.
- Kidner C, Groover A, Thomas D, Emelianova K, Soliz-Gamboa C, Lens F. 2016. First steps in studying the origins of secondary woodiness in Begonia (Begoniaceae): combining anatomy, phylogenetics, and stem transcriptomics. *Biological Journal of the Linnean Society* **117**: 121–138.
- Kitin P, Voelker SL, Meiner FC, Beeckman H, Strauss SH, Lachenbruch B. 2010. Tyloses and phenolic deposits in xylem vessels impede water transport in low-lignin transgenic poplars: study by cryo-fluorescence microscopy. *Plant Physiology* **154**: 887–898.
- Kocacinar F, Sage RF. 2003. Photosynthetic pathway alters xylem structure and hydraulic function in herbaceous plants. *Plant, Cell & Environment* **26**: 2015–2026.
- Kolb KJ, Sperry JS. 1999. Differences in drought adaptation between subspecies of Sagebrush (*Artemisia tridentata*). *Ecology* **7**: 2373–2384.
- Lamy J, Delzon S, Bouche PS, et al. 2013. Limited genetic variability and phenotypic plasticity detected for cavitation resistance in a Mediterranean pine. *New Phytologist* **201**: 874–886.
- Larter M, Brodribb T, John PS, Burrett R, Cochard H, Delzon S. 2015. Extreme aridity pushes trees to their physical limits. *Plant Physiology* **168**: 804–807.
- Lens F, Luteyn JL, Smets E, Jansen S. 2004. Ecological trends in the wood anatomy of Vaccinioideae (Ericaceae s.l.). *Flora* **199**: 309–319.
- Lens F, Sperry JS, Christman MA, Choat B, Rabaey D, Jansen S. 2011. Testing hypotheses that link wood anatomy to cavitation resistance and hydraulic conductivity in the genus *Acer*. *New Phytologist* **190**: 709–723.
- Lens F, Eekhout S, Zwartjes R, Smets E, Janssens S. 2012a. The multiple fuzzy origins of woodiness within Balsaminaceae using an integrated approach. Where do we draw the line? *Annals of Botany* **109**: 783–799.
- Lens F, Smets E, Melzer S. 2012b. Stem anatomy supports *Arabidopsis thaliana* as a model for insular woodiness. *New Phytologist* **193**: 12–17.
- Lens F, Tixier A, Cochard H, Sperry JS, Jansen S, Herbette S. 2013. Embolism resistance as a key mechanism to understand adaptive plant strategies. *Current Opinion in Plant Biology* **16**: 287–292.
- Lens F, Picon-Cochard C, Delmas C, et al. 2016. Herbaceous angiosperms are not more vulnerable to drought-induced embolism than angiosperm trees. *Plant Physiology* **172**: 661–667.
- Li S, Lens F, Espino S, et al. 2016. Intervessel pit membrane thickness as a key determinant of embolism resistance in angiosperm xylem. *IAWA Journal* **37**: 152–171.
- Maherali H, Pockman WT, Jackson R. 2004. Adaptive variation in the vulnerability of woody plants to xylem cavitation. *Ecology* **85**: 2184–2199.
- Maherali H, Walden AE, Husband BC. 2009. Genome duplication and the evolution of physiological responses to water stress. *New Phytologist* **184**: 721–731.
- Martinez-Vilalta J, Cochard H, Mencuccini M, et al. 2009. Hydraulic adjustment of Scots pine across Europe. *New Phytologist* **184**: 353–364.
- Martinez-Vilalta J, Mencuccini M, Vayreda J, Retana J. 2010. Interspecific variation in functional traits, not climatic differences among species ranges, determines demographic rates across 44 temperate and Mediterranean tree species. *Journal of Ecology* **98**: 1462–1475.
- Mencuccini M, Comstock J. 1999. Variability in hydraulic architecture and gas exchange of common bean (*Phaseolus vulgaris*) cultivars under well-watered conditions: interactions with leaf size. *Australian Journal of Plant Physiology* **26**: 115–124.
- Mendiburu F. 2017. *Agricolae: statistical procedures for agricultural research*. R package version 1.2–8. <https://CRAN.R-project.org/package=agricolae> (18 June 2018).
- Monfreda C, Ramankutty N, Foley JA. 2008. Farming the planet: 2. Geographic distribution of crop areas, yields, physiological types, and net primary production in the year 2000. *Global Biogeochemical Cycles* **22**: Gb1022.
- Nolf M, Pagitz K, Mayr S. 2014. Physiological acclimation to drought stress in *Solidago canadensis*. *Physiologia Plantarum* **150**: 529–539.
- Nolf M, Rosani A, Ganthaler A, Beikircher B, Mayr S. 2016. Hydraulic variation in three *Ranunculus* species. *Plant Physiology* **170**: 2085–2094.
- O'Brien MJ, Engelbrecht BMJ, Joswig J, et al. 2017. A synthesis of tree functional traits related to drought induced mortality in forests across climatic zones. *Journal of Applied Ecology* **54**: 1669–1686.
- Oksanen J, Guillaume Blanchet F, Kindt R, et al. 2015. *Vegan: community ecology package*. R package version. <http://CRAN.R-project.org/package=vegan> (11 June 2018).
- Olson ME, Rosell JA. 2013. Vessel diameter–stem diameter scaling across woody angiosperms and the ecological causes of xylem vessel diameter variation. *New Phytologist* **197**: 1204–1213.
- Olson ME, Soriano D, Rosell JA, et al. 2018. Plant height and hydraulic vulnerability to drought and cold. *Proceedings of the National Academy of Sciences, USA* **115**: 7551–7556.
- Pammenter NW, van der Willigen C. 1998. A mathematical and statistical analysis of the curves illustrating vulnerability of xylem to cavitation. *Tree Physiology* **18**: 589–593.
- Pereira L, Domingues-Junior AP, Jansen S, Choat B, Mazzafera P. 2017. Is embolism resistance in plant xylem associated with quantity and characteristics of lignin? *Trees* **32**: 349–358.
- Pinhoiro J, Bates D, DebRoy S, Sarkar D, R Core Team. 2018. *nlme: linear and nonlinear mixed effects models*. R package version 3.1–137. <https://CRAN.R-project.org/package=nlme> (26 June 2018).
- Pittermann J, Choat B, Jansen S, Stuart SA, Lynn L, Dawson TE. 2010. The relationships between xylem safety and hydraulic efficiency in the Cupressaceae: the evolution of pit membrane form and function. *Plant Physiology* **153**: 1919–1931.
- Pivovarov AL, Pasquini SC, Guzman ME, Alstad KP, Stemke JS, Santiago LS. 2016. Multiple strategies for drought survival among woody plant species. *Functional Ecology* **30**: 517–526.
- Poorter L, McDonald I, Alarcón A, et al. 2010. The importance of wood traits and hydraulic conductance for the performance and life history strategies of 42 rainforest tree species. *New Phytologist* **185**: 481–492.
- Pratt RB, Jacobsen AL. 2017. Conflicting demands on angiosperm xylem: tradeoffs among storage, transport and biomechanics. *Plant, Cell & Environment* **40**: 897–913.
- Preston KA, Cornwell WK, Denoyer J. 2006. Wood density and vessel traits as distinct correlates of ecological strategy in 51 California coast range angiosperms. *New Phytologist* **170**: 807–818.
- R Core Team. 2017. *R: a language and environment for statistical computing*. Vienna, Austria: R Foundation for Statistical Computing, <http://www.R-project.org> (11 June 2018).
- RStudio Team. 2016. *RStudio: integrated development for R*. Boston: RStudio, Inc. <http://www.rstudio.com/> (11 June 2018).
- Rahmstorf S, Coumou D. 2012. A decade of weather extremes. *Nature Climate Change* **2**: 491–496.
- Rosenthal DM, Stiller V, Sperry JS, Donovan LA. 2010. Contrasting drought tolerance strategies in two desert annuals of hybrid origin. *Journal of Experimental Botany* **61**: 2769–2778.
- Scholz A, Klepsch M, Karimi Z, Jansen S. 2013. How to quantify conduits in wood? *Frontiers in Plant Science* **56**: 1–11.
- Schreiber SG, Hacke UG, Hamann A. 2015. Variation of xylem vessel diameter in a wide-spread boreal forest tree in western Canada: insights from a large-scale reciprocal transplant experiment. *Functional Ecology* **29**: 1392–1401.
- Schweingruber FH, Borner A, Schulze ED. 2011. *Atlas of stem anatomy in herbs, shrubs and trees*, Vol. 1. Heidelberg: Springer.
- Skelton RP, Brodribb TJ, Choat B. 2017. Casting light on xylem vulnerability in an herbaceous species reveals a lack of segmentation. *New Phytologist* **214**: 561–569.
- Stiller V, Sperry JS. 2002. Cavitation fatigue and its reversal in sunflower (*Helianthus annuus* L.). *Journal of Experimental Botany* **53**: 1155–1161.
- Thorntwaite CW. 1948. An approach toward a rational classification of climate. *Geographical Review* **38**: 55–94.
- Tixier A, Cochard H, Badel E, Dusotoit-Coucaud A, Jansen S, Herbette S. 2013. *Arabidopsis thaliana* as a model species for xylem hydraulics: does size matter? *Journal of Experimental Botany* **64**: 2295–2305.

- Trueba S, Pouteau R, Lens F, *et al.* 2017. Vulnerability to xylem embolism as a major correlate of the environmental distribution of rainforest species on a tropical island. *Plant, Cell & Environment* **40**: 277–289.
- Tyree MT, Sperry JS. 1989. Vulnerability of xylem to cavitation and embolism. *Annual Review of Plant Physiology and Plant Molecular Biology* **40**: 19–38.
- Tyree MT, Zimmermann MH. 2002. *Xylem structure and the ascent of sap*, 2nd edn. Berlin: Springer-Verlag.
- UNEP. 1997. *World atlas of desertification*. Nairobi, Kenya: United Nations Environmental Program.
- Urli M, Porté AJ, Cochard H, Guengant Y, Burlett R, Delzon S. 2013. Xylem embolism threshold for catastrophic hydraulic failure in angiosperm trees. *Tree Physiology* **33**: 672–683.
- Voltaire F, Lens F, Cochard H, *et al.* 2018. Embolism and mechanical resistances play a key role in dehydration tolerance of a perennial grass *Dactylis glomerata* L. *Annals of Botany* **122**: 325–336.
- Wortemann R, Herbette S, Barigah TS, *et al.* 2011. Genotypic variability and phenotypic plasticity of cavitation resistance in *Fagus sylvatica* L. across Europe. *Tree Physiology* **31**: 1175–1182.
- Zanne AE, Westoby M, Falster DS, *et al.* 2010. Angiosperm wood structure: global patterns in vessel anatomy and their relation to wood density and potential conductivity. *American Journal of Botany* **97**: 207–215.
- Zhang YJ, Rockwell FE, Graham AC, Alexander T, Holbrook M. 2016. Reversible leaf collapse: a potential ‘circuit breaker’ against cavitation. *Plant Physiology* **172**: 2261–2274.
- Zieminska K, Butler DW, Gleason SM, Wright IJ, Westoby M. 2013. Fibre wall and lumen fractions drive wood density variation across 24 Australian angiosperms. *Annals of Botany* **5**: 1–14.
- Zuur AF, Ieno EN, Smith GM. 2007. *Analysing ecological data*. New York: Springer Science.
- Zuur AF, Ieno EN, Elphick CS. 2010. A protocol for data exploration to avoid common statistical problems. *Methods in Ecology and Evolution* **1**: 3–14.